

1 **Brief Communication: Recent estimates of glacier mass loss for** 2 **western North America from laser altimetry**

3 Brian Menounos^{1,2,3*}, Alex Gardner⁴, Caitlyn Forentine⁵, Andrew Fountain⁶

4
5 ¹University of Northern British Columbia, Geography Earth and Environmental Sciences, Prince George BC, V2N 4Z9,
6 Canada

7 ²Hakai Institute, Campbell River, BC, Canada

8 ³Geological Survey of Canada - Pacific, Sidney, BC, Canada

9 ⁴Jet Propulsion Laboratory, California Institute of Technology, Pasadena, CA 91109, USA

10 ⁵United States Geological Survey Northern Rocky Mountain Science Center, Bozeman, MT, USA

11 ⁶Portland State University, Department of Geology, Portland, OR, 97201, USA

12
13 *Corresponding author: menounos@unbc.ca

14
15 *Correspondence to:* Brian Menounos (menounos@unbc.ca)

16 **Abstract.** Glaciers in Western North American outside of Alaska are often overlooked in global studies, because their
17 potential to contribute to changes in sea level is small. Nonetheless, these glaciers represent important sources of freshwater,
18 especially during times of drought. Differencing recent ICESat-2 data from a digital elevation model derived from a
19 combination of synthetic aperture radar data (TerraSAR-X/TanDEM-X), we find that over the period 2013-2021, glaciers in
20 western North America lost mass at a rate of -12.3 ± 3.5 Gt yr⁻¹. This rate is comparable to the rate of mass loss (-11.7 ± 1.0
21 Gt yr⁻¹) for the period 2018-2022 calculated through trend analysis using ICESat-2 and Global Ecosystems Dynamics
22 Investigation (GEDI) data.

23 **1 Introduction**

24 Western North American glaciers outside of Alaska cover 14,384 km² of mountainous terrain (Pfeffer et al. 2014). Although
25 the global sea level equivalent of these glaciers is only 2.6 ± 0.7 mm (Farinotti et al., 2019), these glaciers provide important
26 thermal buffering capacity during late summer or during times of drought (Moore et al., 2009). Early attempts to define
27 regional estimates of glacier mass change suffered from sparse, in-situ glaciological observations, non-uniform distribution
28 of geodetic measurements, and uncertainties in gravimetric assessments due to changes in seasonal water storage (Jacob et
29 al., 2012; Gardner et al., 2013; Zemp et al., 2019). Two recent studies combined publicly-available geodetic datasets and
30 statistical methods to yield mass change estimates with much less spatial bias and lower overall uncertainties (Menounos et
31 al., 2019; Hugonnet et al., 2021). Both of these studies rely on DEMs generated from NASA's Advanced Spaceborne
32 Thermal Emission and Reflection Radiometer (ASTER) sensor aboard the Terra satellite. Unfortunately, Terra's orbit is
33 degrading and will reach its end of life within the next 3-4 years (<https://terra.nasa.gov/>). Additional datasets are thus
34 required to quantify glacier mass loss in mountain environments where glacier loss is accelerating (Hugonnet et al., 2021),
35 but the glaciers of western North America have so far been excluded from global altimetry assessments (Jakob and
36 Gourmelen, 2023). Eight of the 19 regions of the globally complete Randolph Glacier Inventory (RGI) are sparsely
37 glacierized, including Western North America. Models and current ice volume estimates suggest that these regions will each
38 contribute ≤ 2 mm to sea level by 2100 under a +2° C global mean temperature warming scenario (Rounce et al. 2023).
39 Several of these regions were not assessed by Jakob and Gourmelen (2023) due to the small size of the glaciers within these

40 regions and complex topography that makes CryoSat-2 processing challenging due in part to the larger beam diameter of
41 CryoSat-2 (~ 380 m) compared to IceSat-2 (~12 m). Here we provide new estimates of recent glacier mass loss based on
42 laser altimetry data for the western United States and Canada which is Region 02 of the Randolph Glacier Inventory (Pfeffer
43 et al., 2014).

44 **2 Data and methods**

45 **2.1 Altimetric data (ICESat-2 and GEDI)**

46 Altimetric data include observations made by NASA's Advanced Topographic Laser Altimeter System (ATLAS), which is a
47 532 nm photon-counting laser system aboard the ICESat-2 satellite that operates in latitudes between 88° N/S (Markus et al.,
48 2017). We use version 5 of the ATL06 (land-ice surface heights) dataset that includes laser shots from 13 October 2018 to 12
49 October, 2022. We also used Global Ecosystem Dynamics Investigation (GEDI) laser data (Liu et al., 2021) acquired
50 between 1 January, 2018 and 1 January, 2022 (GEDI02_A release 2). GEDI is a 1064 nm, full-waveform laser that, because
51 of its operation aboard the International Space Station, operates in latitudes between 51.6° N/S.

52 **2.2 Digital elevation model**

53 The mass change estimate for approximately the last decade (2013 to 2020), herein referred to as the decadal estimate, uses
54 the global, 30 m Copernicus DEM elevation data derived from the TanDEM-X Synthetic Aperture Radar (SAR) mission
55 (Rizzoli et al., 2017) and made publicly available as the Glo30 product, herein referred to as COP-30
56 (<https://spacedata.copernicus.eu/collections/copernicus-digital-elevation-model>). Acquisition of the data used in COP-30
57 DEM occurred between 2010 and early 2015 and coverage represented about five individual SAR tiles in our study region.
58 Because no gridded acquisition date exists for COP-30, we use an acquisition date of 2013, which coincides with the
59 midpoint for the majority of DEM acquisitions (Rizzoli et al., 2017). As described below, we use the ambiguity of DEM
60 acquisition dates as one source of uncertainty in our mass change estimate. Another source of uncertainty is penetration of
61 the TanDEM-X radar signal into high elevation firn and snow surfaces (Abdullahi et al., 2019). As described in the
62 discussion section of our paper, we consider the magnitude of this bias to be small.

63
64 For each subregion, we reprojected the COP-30 into the respective UTM zone of a given subregion. The COP-30 vertical
65 datum is EGM96 which we converted to match the vertical datum of ICESat-2 (WGS84). We clipped ICESat-2 data for a
66 given acquisition date to a region of interest and extracted the closest grid point of the COP-30 data for a given laser shot.
67 Retained data include elevation of both COP-30 and ICESat-2, derived elevation change [m] and rates of elevation change
68 [m yr⁻¹]. We also include other original attributes present with the ICESat-2 data (e.g. track number, effective laser shot
69 radius, slope) to maintain metadata continuity. Excluded elevation change values exceeded elevation change rates of -20 or
70 20 m yr⁻¹ since we assumed that these signals exceed the range of what is physically attributable to glacier processes. To our
71 knowledge, we know of no glaciers in WNA that experience surging or advance over the past two decades (Bevington and
72 Menounos, 2021; Fountain et al., 2023).

73
74 For the decadal estimate of mass change, we buffered each glacier polygon (RGI ver. 6.0) within the study region by 1 km
75 and then masked from the original glacier polygon, to capture areas adjacent to glaciers that we considered to be areas of
76 stable terrain. This stable terrain might include vegetated terrain, landslides or standing water, however. Due to the buffer,
77 we expect results to be robust to glacier polygon updates. Note that the recently released RGI-7.0 has no changes from RGI-
78 6.0 in our study area. Inspection of elevation change over stable terrain for all ICESat-2 laser shots (2.24×10^6) reveals a
79 positive bias for almost every subregion, typically on the order of 0.1-0.5 m yr⁻¹ (ICESat-2 minus COP-30); this bias,
80 however, did not substantially vary with elevation for a given region. Visual inspection of elevation change maps and review
81 of acquisition dates of ICESat-2 data suggests this positive bias arises by laser shots over snow-covered terrain (c.f. Enderlin

82 et al., 2022). We therefore limit our analysis to the ablation season when the positive bias associated with snow-covered
83 terrain is minimized. Confirmation of the source of this bias is revealed when the analysis of rates of elevation change is
84 limited to ICESat-2 laser shots acquired between 1 August and 1 October. For these late summer laser shots, we respectively
85 observe a mean bias and uncertainty (± 1 sigma) over stable terrain of 0.038 and 1.53 m yr⁻¹.

86 2.3 Recent rate of elevation change from ICESat-2 and GEDI

87 For the period 2018-2022, herein referred to as the recent period, we first create altimetry anomalies by differencing ICESat-
88 2 and GEDI laser shots to the COP-30 DEM. A least squares regression that includes an offset, trend and seasonal sinusoidal
89 terms is fit to anomalies within a 250 m radius search window. The y-intercept of the regression is set to the year 2020. We
90 exclude any ICESat-2 or GEDI laser shots if they deviate more than 250 m from the COP-30 DEM, or if they deviate by
91 more than 150 m from the median anomaly within the 250 m search radius. The search radius and median anomaly threshold
92 were selected to omit elevation change signals that were not physically realistic. Regression fits were excluded from further
93 analysis if: (i) there were fewer than five data point for given search window; (ii) the temporal span of observations is less
94 than three years; (iii) the root mean squared error (RMSE) of the fit residuals exceed 5.0 m yr⁻¹ and (iv); the seasonal
95 amplitude of the least squares fit exceeds 10 m yr⁻¹. We use the trend obtained from the regression to the 250 m radius to
96 represent elevation change. This filtering yielded an unbiased sample across elevation bins of ice in study area (i.e. the area
97 distributions of sampled vs. observed ice were similar).
98

99 2.4 Mass change uncertainty

100 Uncertainty in mass change originates from errors in rates of elevation change and volume-to-mass conversion factor. We
101 use 850 kg m⁻³ and its associated uncertainty term (± 60 kg m⁻³) for mass conversion (Huss, 2013). We generate bootstrapped
102 errors in total volume change using a Monte Carlo method. We first temporally randomize the laser altimetric data, randomly
103 choose the acquisition date of the COP-30 DEM (2012, 2013, 2014) and sample 5% of the data with replacement 1,000
104 times. Total volume change over glacierized terrain is calculated for each synthetic dataset by multiplying the rate of
105 elevation change by the area of glaciers within a given elevation bin (100 m bins). We then take 5% and 95% modelled
106 volume change as our uncertainty.
107

108 Uncertainty in mass change is then calculated from:
109

$$110 \sqrt{(dV_{\sigma} \cdot \rho)^2 + (\rho_{\sigma} \cdot dV)^2} \quad (1)$$

111 Where dV_{σ} is the uncertainty of volume change generated from the Monte Carlo method, ρ is material density (850 kg m⁻³),
112 ρ_{σ} is uncertainty of density (60 kg m⁻³) and dV is the change in volume.
113

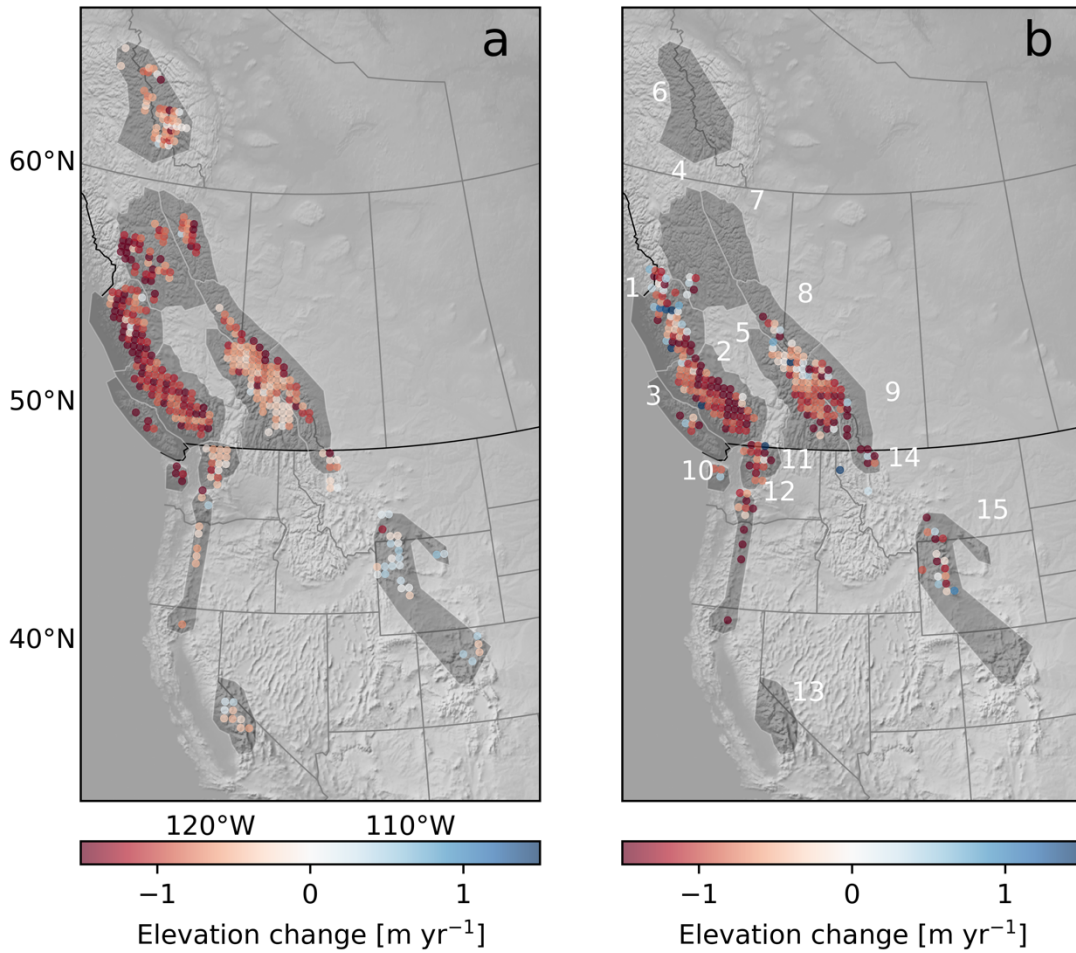
114 3.0 Results

115 To minimize the impact of the seasonal snow signal, we limit the presentation of our analysis to mass change using ICESat-2
116 and COP-30 elevation changes to ICESat-2 data acquired during the latter half of the ablation season (1 August - 1 October).
117 Glaciers throughout the western United States and Canada thinned both during the decadal and recent period with prominent
118 thinning within the Southern Coast Mountains, a region that contains nearly one half of the total ice cover of the study region
119 (Fig. 2). For the period 2013-2021 (median date of ICESat-2 data is 26 August, 2020), we estimate a rate of mass change of
120 -12.3 ± 3.5 Gt yr⁻¹ (Fig. 1). This measurement agrees within the rate of mass change $[-12.3 \pm 4.6$ Gt yr⁻¹] reported for the
121 period 2009–2018 (Menounos et al., 2019) and the estimate $[-12.3 \pm 3.0$ Gt yr⁻¹] for the period 2015-2019 based primarily
122 on ASTER data (Hugonnet et al., 2021). Comparable estimates of mass loss exist for western North America for the period
123 1961-2016 $[-12 \pm 6$ Gt yr⁻¹] and for the period 2002-2009 $[-14 \pm 3$ Gt yr⁻¹] respectively from Zemp et al., (2019) and Gardner
124 et al., (2013). Using only ICESat-2 and GEDI laser shots and rates of elevation change determined through least squares
125 fitting (i.e. the recent period), glaciers lost -11.7 ± 1.0 Gt yr⁻¹ of mass for the period 2018-2022 (Fig. 2). Mass change rates

126 per subregions (Fig. 1) are summarized in the supplementary material (SM Table 1). The effect of a small sample size is
127 evident in the larger uncertainty of elevation change at highest and lowest elevations, but the contribution of this error to
128 total mass change is small since little total glacierized area exists at these elevations.

129 **4.0 Discussion and Conclusion**

130 Our geodetic balance obtained from laser altimetry using least squares fitting provides the most recent mass change update
131 for western North America, a region excluded in a recent global assessment of glacier mass loss using laser altimetry from
132 CryoSat-2 data (Jakob and Gourmelen, 2023). While our trend analysis provides a robust estimate of recent glacier mass
133 change, insufficient sampling precludes our assessment of mass loss for regions where laser altimetry data are sparse. This
134 sparseness is especially pronounced in regions north of GEDI data coverage (51.6° N), e.g. Nahanni, and regions
135 characterised by very small glaciers, e.g. Sierra Nevada (Fig. 2). Our decadal estimates of glacier mass loss provide insight
136 into sub-regional patterns of glacier mass loss, but insight is offset by the additional uncertainty of radar penetration at
137 highest elevation and the ambiguity of the acquisition data for the COP-30 DEM. Others report penetration of the TanDEM-
138 X radar signal into high elevation firn and snow surfaces (Abdullahi et al., 2019). The potential of this penetration bias to
139 greatly affect our results is limited since it is spatially limited to highest elevation zones containing dry snow and firn (Millan
140 et al., 2015); these zones typically represent $< 1\text{-}2\%$ of the total glacierized area within a given region of this study.

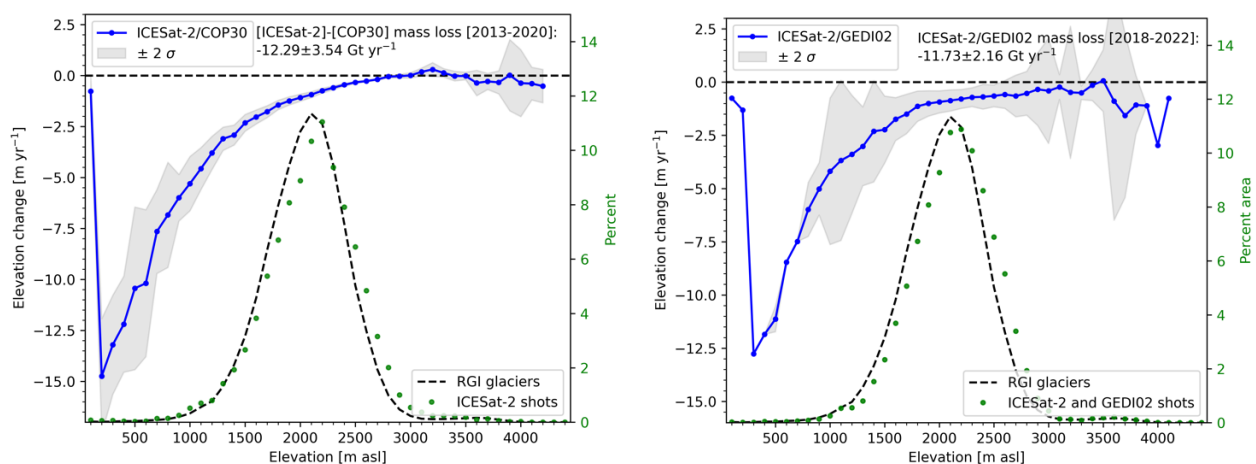


141
 142 **Figure 1: Elevation change [m yr⁻¹] for western North American glaciers. Data are aggregated to points with 50 km spacing. Left**
 143 **panel (a): Elevation change [m yr⁻¹] determined from ICESat-2 and COP-30 data (2020 - 2013); Right Panel (b): Elevation change**
 144 **[m yr⁻¹] from trend analysis over period 2022-2018 from ICESat-2 and GEDI laser altimetric data. Numbers refer to glacierized**
 145 **regions of Western North America (RGI region 02). The regions include: (1) Central Coast (1,692 km²); (2) Southern Coast (7,181**
 146 **km²); (3) Vancouver Island (15 km²); (4) Northern Interior (572 km²); (5) Southern Interior (1,959 km²); (6) Nahanni (657 km²);**
 147 **(7) Northern Rocky Mountains (415 km²); (8) Central Rocky Mountains (422 km²); (9) Southern Rocky Mountains (1,350 km²);**
 148 **(10) Olympics (30 km²); (11) North Cascades (250 km²); (12) South Cascades (153 km²); (13) Sierra Nevada (11 km²); (14) Glacier**
 149 **National Park (11 km²) and; (15) Wind River (60 km²).**
 150
 151

152 The regional pattern of elevation change obtained for the recent period shows areas of neutral or slight elevation gain (e.g.
 153 regions 1 and 5) that are not apparent in the map of decadal elevation change (Fig. 1). The most parsimonious explanation
 154 for these differences is the influence of spatially variable snow accumulation in these regions, though we cannot rule out the
 155 possibility of changing balance between ice dynamics and mass balance to explain the observed elevation changes. In
 156 addition, the decadal pattern largely accords with the notable zonal difference in elevation change observed by Menounos et
 157 al., (2019). A key finding of Hugonnet et al., (2021) was the notable accelerated mass loss in western North America during
 158 the period 2015-2019 relative to the start of the 21st century. Our decadal results are consistent in both magnitude and
 159 uncertainty to previous estimates using instruments (i.e. ASTER) that will soon be unavailable, and so our approach assures

160 mass change estimates can be obtained using much sparser observations from laser altimetry. Our recent and decadal
161 estimates of glacier mass loss using independent datasets confirms the magnitude of recent mass change for a comparably
162 recent period (2018 to 2022), corroborating the finding of accelerated mass loss from this previous study.
163

164 Glaciers in western North America provide cold meltwater that buffers hot and dry conditions (Anderson and Radić, 2020;
165 Moore et al., 2009), sustains alpine stream ecosystems (e.g. Muhlfield et al., 2020), and supports downstream communities
166 via agricultural irrigation and hydroelectric power generation (e.g. Frans et al., 2018). Thus, our study provides relevant,
167 detailed information to land managers who are responsible for understanding and responding to the local consequences of
168 rapid glacier change. Sparsely glacierized regions in Western North America and Europe contribute minimally to sea level
169 change (Rounce et al., 2023) but coincide with river basins where mountain water supply and downstream demand are
170 highest (Immerzeel et al., 2019). This justifies the need to surmount technical and data limitations that impede quantifying
171 glacier mass change in sparsely glacierized regions. The projected, continued loss of glacier ice (Rounce et al. 2023)
172 furthermore suggests that this technical challenge will only become more widespread.
173



176
177
178
179
180 **Figure 2: In both panels, light grey shading denotes uncertainty (5-95%) of elevation change. Black dashed line and green dots,**
181 **respectively, indicate percent area of RGI ice and percentage of ICESat-2 laser shots within a given elevation bin. Left Panel:**
182 **Rates of elevation change [m yr⁻¹] versus elevation for the period 2013-2020. Only laser shots from 1 August-1 October (n=347,630)**
183 **used in analysis. Right Panel: Rates of elevation change [m yr⁻¹] versus elevation for the period 2018-2022 from ICESat-2 and**
184 **GEDI laser shots from least-squares trend analysis (n=66,201).**
185

186 Code and data availability

187 Available upon request from the authors.

189 Declaration of competing interest

190 The authors declare that they have no competing interests that influenced the research presented in this publication.
191

192

193 **Author contribution**

194 BM proposed the study. BM and AG analyzed the data and wrote the original draft. All authors provided feedback on the
195 initial draft of the manuscript and contributed to the final writing and editing of the paper.

196

197

198 **Acknowledgements**

199 The authors acknowledge constructive input from Rainey Aberle, Albin Wells, Erik Mannerfelt and an anonymous referee
200 which improved the quality and clarity of this manuscript. Menounos acknowledges support from the National Research and
201 Engineering Council of Canada, the Tula Foundation. Florentine acknowledges support from the U.S. Geological Survey
202 Ecosystem Mission Area Climate Research and Development Program. Any use of trade, firm, or product names is for
203 descriptive purposes only and does not imply endorsement by the U.S. Government.
204

205 **References**

206 Abdullahi, S., Wessel, B., Huber, M., Wendleder, A., Roth, A., and Kuenzer, C.: Estimating Penetration-Related X-Band
207 InSAR Elevation Bias: A Study over the Greenland Ice Sheet, *Remote Sensing*, 11, 2903, 2019.

208 Anderson, S., Radić, V. Identification of local water resource vulnerability to rapid deglaciation in Alberta. *Nat. Clim.*
209 *Chang.* 10, 933–938 (2020)

210 Bevington, A., and Menounos, B. Accelerated change in the glaciated environments of western Canada revealed through
211 trend analysis of optical satellite imagery, *Remote Sensing of Environment*, 270, 2022.

212 Enderlin, E. M., Elkin, C. M., Gendreau, M., Marshall, H. P., O’Neel, S., McNeil, C., Florentine, C., and Sass, L.:
213 Uncertainty of ICESat-2 ATL06- and ATL08-derived snow depths for glacierized and vegetated mountain regions, *Remote*
214 *Sens. Environ.*, 283, 113307, 2022.

215 Farinotti, D., Huss, M., Fürst, J. J., Landmann, J., Machguth, H., Maussion, F., and Pandit, A.: A consensus estimate for the
216 ice thickness distribution of all glaciers on Earth, *Nat. Geosci.*, 12, 168–173, 2019.

217 Fountain, A. G., Glenn, B., and McNeil, C.: Inventory of glaciers and perennial snowfields of the conterminous USA, *Earth*
218 *Syst. Sci. Data*, 15, 4077–4104, <https://doi.org/10.5194/essd-15-4077-2023>, 2023.

219 Frans, C., Istanbuluoglu, E., Lettenmaier, D. P., Fountain, A. G. and Riedel, J.: Glacier Recession and the Response of
220 Summer Streamflow in the Pacific Northwest United States, 1960–2099, *Water Resour. Res.*, 54, 6202–6225, 2018.

221 Gardner, A. S., Moholdt, G., Cogley, J. G., Wouters, B., Arendt, A. A., Wahr, J., Berthier, E., Hock, R., Pfeffer, W. T.,
222 Kaser, G., Ligtenberg, S. R. M., Bolch, T., Sharp, M. J., Hagen, J. O., van den Broeke, M. R., and Paul, F.: A reconciled
223 estimate of glacier contributions to sea level rise: 2003 to 2009, *Science*, 340, 852–857, 2013.

224 Hugonnet, R., McNabb, R., Berthier, E., Menounos, B., Nuth, C., Girod, L., Farinotti, D., Huss, M., Dussaillant, I., Brun, F.,
225 and Kääb, A.: Accelerated global glacier mass loss in the early twenty-first century, *Nature*, 592, 726–731, 2021.

226 Huss, M.: Density assumptions for converting geodetic glacier volume change to mass change, *The Cryosphere*, 7, 877–887,
227 2013.

- 228 Immerzeel, W. W., Lutz, A. F., Andrade, M., Bahl, A., Biemans, H., Bolch, T., Hyde, S., Brumby, S., Davies, B. J., Elmore,
229 A. C., Emmer, A., Feng, M., Fernández, A., Haritashya, U., Kargel, J. S., Koppes, M., Kraaijenbrink, P. D. A., Kulkarni, A.
230 V., Mayewski, P. A., Nepal, S., Pacheco, P., Painter, T. H., Pellicciotti, F., Rajaram, H., Rupper, S., Sinisalo, A., Shrestha,
231 A. B., Viviroli, D., Wada, Y., Xiao, C., Yao, T. and Baillie, J. E. M.: Importance and vulnerability of the world's water
232 towers, *Nature*, 577, 364–369, 2019.
- 233 Jacob, T., Wahr, J., Pfeffer, W. T., and Swenson, S.: Recent contributions of glaciers and ice caps to sea level rise, *Nature*,
234 482, 514–518, 2012.
- 235 Jakob, L. and Gourmelen, N.: Glacier mass loss between 2010 and 2020 dominated by atmospheric forcing, *Geophys. Res.*
236 *Let.*, 50, <https://doi.org/10.1029/2023gl1102954>, 2023.
- 237 Liu, A., Cheng, X., and Chen, Z.: Performance evaluation of GEDI and ICESat-2 laser altimeter data for terrain and canopy
238 height retrievals, *Remote Sens. Environ.*, 264, 112571, 2021.
- 239 Markus, T., Neumann, T., Martino, A., Abdalati, W., Brunt, K., Csatho, B., Farrell, S., Fricker, H., Gardner, A., Harding, D.,
240 Jasinski, M., Kwok, R., Magruder, L., Lubin, D., Luthcke, S., Morison, J., Nelson, R., Neuenschwander, A., Palm, S.,
241 Popescu, S., Shum, C. K., Schutz, B. E., Smith, B., Yang, Y., and Zwally, J.: The Ice, Cloud, and land Elevation Satellite-2
242 (ICESat-2): Science requirements, concept, and implementation, *Remote Sens. Environ.*, 190, 260–273, 2017.
- 243 Menounos, B., Hugonnet, R., Shean, D., Gardner, A., Howat, I., Berthier, E., Pelto, B., Tennant, C., Shea, J., Noh, M.-J.,
244 Brun, F., and Dehecq, A.: Heterogeneous Changes in Western North American Glaciers Linked to Decadal Variability in
245 Zonal Wind Strength, *Geophys. Res. Lett.*, 46, 200–209, 2019.
- 246 Millan, R., Dehecq, A., Trouvé, E., Gourmelen, N., and Berthier, E.: Elevation changes and X-band ice and snow penetration
247 inferred from TanDEM-X data of the Mont-Blanc area, 2015 8th International Workshop on the Analysis of Multitemporal
248 Remote Sensing Images (Multi-Temp), Annecy, France, 2015, pp. 1-4, doi: 10.1109/Multi-Temp.2015.7245753.
- 249 Moore, R. D., Fleming, S. W., Menounos, B., Wheate, R., Fountain, A., Stahl, K., Holm, K., and Jakob, M.: Glacier change
250 in western North America: influences on hydrology, geomorphic hazards and water quality, *Hydrol. Process.*, 23, 42–61,
251 2009.
- 252 Muhlfeld, C. C., Cline, T. J., Giersch, J. J., Peitzsch, E., Florentine, C., Jacobsen, D. and Hotaling, S.: Specialized meltwater
253 biodiversity persists despite widespread deglaciation, *Proc. Natl. Acad. Sci. U. S. A.*, 117, 2020,
254 doi:10.1073/pnas.2001697117, 2020. Pfeffer, W. T., Arendt, A. A., Bliss, A., Bolch, T., Cogley, J. G., Gardner, A. S., Hagen,
255 J.-O., Hock, R., Kaser, G., Kienholz, C., and Others: The Randolph Glacier Inventory: a globally complete inventory of
256 glaciers, *J. Glaciol.*, 60, 537–552, 2014.
- 257 Rizzoli, P., Martone, M., Gonzalez, C., Wecklich, C., Borla Tridon, D., Bräutigam, B., Bachmann, M., Schulze, D., Fritz, T.,
258 Huber, M., Wessel, B., Krieger, G., Zink, M., and Moreira, A.: Generation and performance assessment of the global
259 TanDEM-X digital elevation model, *ISPRS J. Photogramm. Remote Sens.*, 132, 119–139, 2017.
- 260 Rounce, D. R., Hock, R., Maussion, F., Hugonnet, R., Kochtitzky, W., Huss, M., Berthier, E., Brinkerhoff, D., Compagno,
261 L., Copland, L., Farinotti, D., Menounos, B. and McNabb, R.: Global glacier change in the 21st century: Every increase in
262 temperature matters, *Science*, 379, 78–83, 2023.
- 263 Zemp, M., Huss, M., Thibert, E., Eckert, N., McNabb, R., Huber, J., Barandun, M., Machguth, H., Nussbaumer, S. U.,
264 Gärtner-Roer, I., Thomson, L., Paul, F., Maussion, F., Kutuzov, S., and Cogley, J. G.: Global glacier mass changes and their
265 contributions to sea-level rise from 1961 to 2016, <https://doi.org/10.1038/s41586-019-1071-0>, 2019.